ARTICLES

Dynamics of *p*-Terphenyl Crystals at the Phase Transition Temperature: A Zero-Field EPR Study of the Photoexcited Triplet State of Pentacene in *p*-Terphenyl Crystals

Jun Lang, David J. Sloop, and Tien-Sung Lin*

Department of Chemistry, Washington University, St. Louis, Missouri 63130-4899

Received: January 11, 2007; In Final Form: February 25, 2007

Pulsed zero-field electron paramagnetic resonance free induction decay (ZF EPR FID) techniques are employed to study the phase transition of *p*-terphenyl crystals (T_c = 193 K) by measuring selectively populated photoexcited triplet ZF transitions of dilute pentacene molecules in *p*-terphenyl single crystals. The sensitivity of ZF spectroscopy to small shifts in local magnetic fields enables the studies of guest−host configuration changes over a wide temperature range. Here we report the observation of guest pentacene (-h_{14} and -d_{14}) triplet ZF EPR FID spectra that disappear abruptly at T_c and of spectral broadening and shift below T_c. We interpret these spectral changes as evidence for guest couplings to host phenyl rings. Further, these data allow assignments of spectroscopic sites to crystallographic sites that occur in the phase transition.

Introduction

At room temperature, the two outer phenyl rings of the *p*-terphenyl molecule in the crystalline phase lie in the same plane, and the central ring undergoes a rapid rocking motion with an amplitude of 15° with respect to the outer phenyl rings.[1−3] This motion arises from the competition between π-electron delocalization and the repulsion among the ortho-hydrogens of neighboring phenyl rings. Because the shape and the size of pentacene molecules are about the same as those of *p*-terphenyl molecules, a small percentage of pentacene molecules can substitute for *p*-terphenyl molecules at lattice sites to give a uniform, dilute mixed organic crystal. At 193 K, a phase transition takes place as the crystal structure changes from the monoclinic phase (space group $P2_1/a$, 2 molecules/cell) to triclinic (space group $P\bar{1}$, 4 molecules/cell). Consequently, for temperatures below T_c, the central phenyl ring and the outer rings of *p*-terphenyl crystals are "frozen" (motional slowdown), which leads to four sites that are distinguishable by differing central phenyl ring to outer ring angles. Below T_c, pentacene molecules occupy four inequivalent sites in the crystal. From an analysis of spectral diffusion observed in the single molecule spectroscopy studies of pentacene in *p*-terphenyl, it was reported that the electronic transition frequency of pentacene is modulated by reorientation of the central phenyl ring even at very low temperatures.[4−6] Therefore, the conformation changes of host *p*-terphenyl molecules might well be expected to have substantial effects on the molecular and the electronic structures of the surrounding guest pentacene molecules at a given temperature.

Here we report a study of zero-field electron paramagnetic resonance (ZF EPR) spectral changes of the photoexcited triplet state of pentacene molecules as the host *p*-terphenyl crystal traverses T_c. Previously, we reported the ZF EPR spectra of the pentacene triplet in *p*-terphenyl are typically narrower than 700 kHz.[7] The narrow spectral line width is attributed to the vanishing first-order hyperfine interaction (HFI) in ZF. Transitions among triplet sublevels (T_x, T_y, and T_z) in ZF can therefore be measured to within 10 kHz (10 ppm) by ZF EPR experiments. Furthermore, high electron spin polarization, long relaxation times, and long lifetimes of the photoexcited triplet state of pentacene in *p*-terphenyl crystals allow relatively high signal-to-noise (S/N) measurements of transient triplet EPR signals over a wide range of temperatures.[8−10] Thus, we apply pulsed ZF EPR to measure photoexcited pentacene triplet ZF transitions as single crystals of doped *p*-terphenyl traverse T_c in attempts to document the details of associated guest−host conformation changes.

The process of cooling crystal samples below T_c results in changing the net alignments of *p*-terphenyl central phenyl rings with respect to their associated outer rings. Hence, this phase transition has been characterized as an order−disorder transition. In fact, Baudour et al. proposed a double-well potential model to characterize the phase transition.[1,3] Baudour et al. also determined that the low-temperature phase of *p*-terphenyl has four inequivalent sites that are distinguished by the angle between the central phenyl ring and the outer rings (designated as M_1, M_2, M_3, and M_4).[11] On the other hand, Kryschi et al. calculated pentacene equilibrium conformations in each of the four triclinic *p*-terphenyl sites (designated as P_1, P_2, P_3, and P_4 sites) based on molecular packing calculations, and they discovered that pentacene molecules are nearly planar in two of the four sites (P_3 and P_4), whereas they are distorted to nonplanar in the other two sites (P_1 and P_2).[11] Unfortunately, Kryschi et al. did not clarify the correspondence between the two different nomenclatures of crystal sites: P_1−P_4 and M_1−M_4.

The existence of inequivalent sites was also observed in the fluorescence spectrum of pentacene-h_{14} in *p*-terphenyl taken at liquid helium temperatures; four different transition origins

* Author to whom correspondence should be addressed. E-mail: Lin@wustl.edu.

10.1021/jp070251v CCC: $37.00
Published on Web 05/11/2007

(spectroscopic sites) were observed at 16 883, 16 887, 17 006, and 17 065 cm^{-1}, which were referred to as O_1, O_2, O_3, and O_4, respectively.[12−16] Köhler et al. reported an optically detected magnetic resonance (ODMR) study of the system by monitoring the fluorescence intensity as a function of microwave frequency where they observed four inequivalent spectroscopic sites O_1, O_2, O_3, and O_4, for each of the T_x-T_z and T_y-T_z transitions at 1.2 K.[17] There has been an ongoing debate regarding assignments between spectroscopic sites and crystalline sites of pentacene in *p*-terphenyl crystals.[11,15,17−19] Because our ZF EPR measurements can be performed with excellent precision over a wide range of temperatures, another objective of the present study is therefore to establish the correspondence between the lattice sites and the observed spectral sites.

Experimental Section

The details of the ZF EPR spectrometer and of crystal preparation were previously given.[7,20,21] Two crystal systems are employed in our studies: pentacene-h_{14} in *p*-terphenyl (PHPT) and pentacene-d_{14} in *p*-terphenyl (PDPT). The details of the temperature control were described previously.[21] Briefly, the sample and the microwave resonator were placed inside a quartz Dewar. The phase transition of the *p*-terphenyl crystal was traversed by passing cold nitrogen vapor into the Dewar that contained the sample and the resonator. The temperature was controlled by adjusting electric current that passed through heating resistors inside a liquid nitrogen container. The resonator tuning system was de-iced by blowing dry nitrogen at the top of the Dewar. The temperature of the sample was monitored by two sets of thermocouples, which were placed 2−3 cm above and below the sample. The thermocouple reading accuracy was ±1 °C. During each measurement a stable sample temperature was maintained for 10 min prior to acquiring EPR data.

In a typical ZF EPR experiment, we phase detected, digitized, and averaged 100−500 pentacene triplet FID signals; each followed a timed pulse sequence that consisted of a 5 ns N_2 laser pulse of irradiation, a 100 ns delay, and a 75 ns microwave pulse. Equilibrium recovery time intervals from 1 to 10 s were allowed between each timed pulse sequence.

Results and Discussion

1. Disappearance of the FID Signal at T_c. In numerous attempts, we failed to observe any spin−echo signals with two- or three-pulse timed microwave pulse sequences at sample temperatures above T_c. Lack of an observable spin−echo signal indicated that the ZF FID signal observed at room temperature was homogeneously narrowed and that the system is in a fast motion (site-jumping) regime at higher temperature. The effect is attributed to a large molecular motion that arises from the reorientation of the central phenyl ring of the host *p*-terphenyl molecule and its subsequent effect on the surrounding guest pentacene molecule. In fact, it has been reported that the *p*-terphenyl crystal undergoes an unusually large thermal motion in the disordered phase even at low temperatures.[3,8]

Figure 1 displays the fast Fourier transform (FFT) spectra of the measured ZF FID as a function of temperature in the neighborhood of T_c for the T_x-T_z transition of (a) PHPT and (b) PDPT crystals. We note that the FID spectral intensities disappear abruptly for both crystals at T_c. We speculate that the extreme diminishing of ZF spectral intensity at T_c may arise from the following two factors: (1) the EPR spectra become broader due to a critical slowdown of site-jumping, and (2) the density matrix elements that characterize the creation of detectable magnetization diminish.

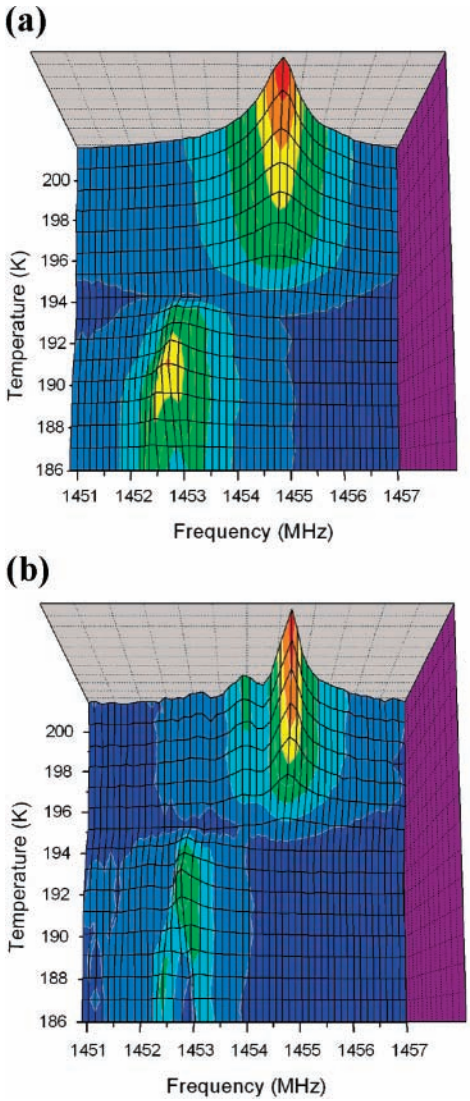

Figure 1. ZF EPR FID FT spectral assemblies as a function of temperature for the T_x-T_z transition of (a) PHPT and (b) PDPT crystals. The signal disappears abruptly at 193 K (T_c).

Let us consider the former factor first. It was pointed out in the X-ray and the neutron studies of *p*-terphenyl crystal structure[1−3] and in the stochastic analysis of fluorescence spectral diffusion of the pentacene molecule dispersed in *p*-terphenyl crystal that the motion of the molecule in the lattice goes from a simple harmonic at room temperature to a more complex motion in a double-well potential below T_c, and a two-level system of the lattice is proposed.[6] Previously, we also reported a spin−echo EPR (x-band) study of both PHPT and PDPT systems as a function of temperature. There we observed some peculiar spectral splittings and shifts at low temperatures (26−160 K). We attributed these spectral behaviors in terms of site-jumping dynamics in the framework of an asymmetric double-well potential.[8] Thus, the changes of the librational motion of *p*-terphenyl molecules in the crystal lattices could affect the structure and the electronic nature of the surrounded pentacene molecule.

Furthermore, in NMR studies of protonated and deuterated *p*-terphenyl crystals, nuclear relaxation rates were measured as a function of temperature, and it was found that proton and deuteron relaxation rates reach maximum values at T_c for each sample.[22,23] The results were explained in terms of critical motion slowing phenomena. It is interesting to note that the central phenyl ring libration frequency is estimated to be

approximately 2.1 THz, or 70 cm^{-1} at temperatures above T_c, but that it may drop to near 100 MHz at T_c.[6] The librational dispersion is 35.2 deg^2 at 200 K, and it increases to 52.5 deg^2 at 298 K.[1] In our ZF experiments, we also observed EPR spectral line width broadening as sample temperatures traverse from above to below T_c. Thus, the extreme slowdown of site-jumping and the further spectral splitting from 2-site (2 inequivalent sites/cell) to 4-site may account for the diminished intensity of ZF EPR FID signals at T_c.

Next we consider the contents of density matrix elements. The magnetic moment of the triplet system is given by the following density matrix in the basis set of ZF spin states, T_x, T_y, and T_z

$$\mu_j(t) = \mathrm{Tr}[S_j\rho(t)] \quad j = x, y, \text{and } z \tag{1}$$

where $\rho(t) = R_{relax}(t)\cdot R_{pulse}(\theta_P)\cdot\rho(0)\cdot R_{pulse}(\theta_P)^+\cdot R_{relax}(t)^+$, $R_{relax}(t) = \exp[-i(H_d + H_{hf})t/\hbar]$, $R_{pulse}(\theta_P) = \exp[-i\, S_j\theta_P/\hbar]$, θ_P is the flipping angle, $\hbar = h/2\pi$, h is Planck's constant, H_d is the Hamiltonian for the dipolar interaction of electron spins, and H_{hf} is the hyperfine interaction between electron and nuclear spins. At $t = 0$, immediately after the photoexcitation

$$\rho(0) = \begin{pmatrix} P_x & 0 & 0 \\ 0 & P_y & 0 \\ 0 & 0 & P_z \end{pmatrix} \tag{2}$$

where P_j is the population rate of the T_j spin state. The populations of the triplet sublevels created by the laser are governed by the molecular symmetry, the spin−orbit coupling, and the guest−host interaction. From eqs 1 and 2, a time dependent magnetic moment along the *y*-axis, $\mu_y(t)$, can be created by applying an S_y operator, which induces the T_x−T_z transition as expressed in the following equation.[7]

$$\mu_y(t) = \mathrm{Tr}[S_y\rho(t)] = -(P_z - P_x)\sin(2\theta_P)\sin\{(Z - X)t\} \tag{3}$$

where X, Y, and Z are the eigenvalues of the ZF spin states. The population ratios of the pentacene triplet are temperature and host dependent.[8,10]

Let us take one step further to examine the off-diagonal density matrix elements modeling time evolution near T_c. After the microwave pulse, the density matrix at time t_b is given as,[21] and $\mu_y(t)$ can be rewritten as follows:

$$\rho(t_b) = \begin{pmatrix} \rho_{xx} & \rho_{xy} & \rho_{xz} \\ \rho_{yx} & \rho_{yy} & \rho_{yz} \\ \rho_{zx} & \rho_{zy} & \rho_{zz} \end{pmatrix} \tag{4}$$

$$\mu_y(t) = \mathrm{Tr}[S_y\rho(t)] = \mathrm{Tr}\left(\begin{pmatrix} 0 & 0 & i \\ 0 & 0 & 0 \\ -i & 0 & 0 \end{pmatrix}\begin{pmatrix} \rho_{xx} & \rho_{xy} & \rho_{xz} \\ \rho_{yx} & \rho_{yy} & \rho_{yz} \\ \rho_{zx} & \rho_{zy} & \rho_{zz} \end{pmatrix}\right) = i(\rho_{zx} - \rho_{xz}) = 2\mathrm{Im}[\rho_{zx}(t)] \tag{5}$$

Note that ρ_{zx} is the complex conjugate of ρ_{xz}, and its value is proportional to the population difference between T_x and T_z as indicated in eq 3. Thus, if $\mathrm{Im}[\rho_{zx}(t)]$ becomes vanishingly small due to the reorientation of the symmetry axis at T_c (particularly for the mixing of *x* and *z* axes as the pentacene distorts out-of-plane), then the off-diagonal element $\rho_{zx}(t)$ could become extremely small, and the ZF FID signal would disappear (see the following section for further discussion).

2. The Spectral Behaviors of the T_x−T_z Transition Below T_c. The ZF spectra that correspond to the T_x−T_z transition at temperatures below T_c for the PHPT sample are displayed in Figure 2 panel a, and those for PDPT are in panel b. Our measurements show that the frequency differences for the T_x−T_z transition between PHPT and PDPT are less than 0.1 MHz. We observe single spectral lines splitting into two resolvable peaks for both samples at temperatures that are immediately below T_c. Thus, EPR spectra that possibly correspond to optical spectroscopic sites are resolved at near T_c temperatures for the first time. We further extended our measurements to 1465 MHz for a different crystal sample (see Figure 3). We note the low-frequency group has a higher intensity and does not shift significantly as the temperature decreases further; the high-frequency group has a lower intensity and shifts rapidly to the blue side of the spectrum as the temperature decreases. We shall establish the correspondence between these two distinct spectral groups and the two groups of planar and nonplanar pentacene conformations below.

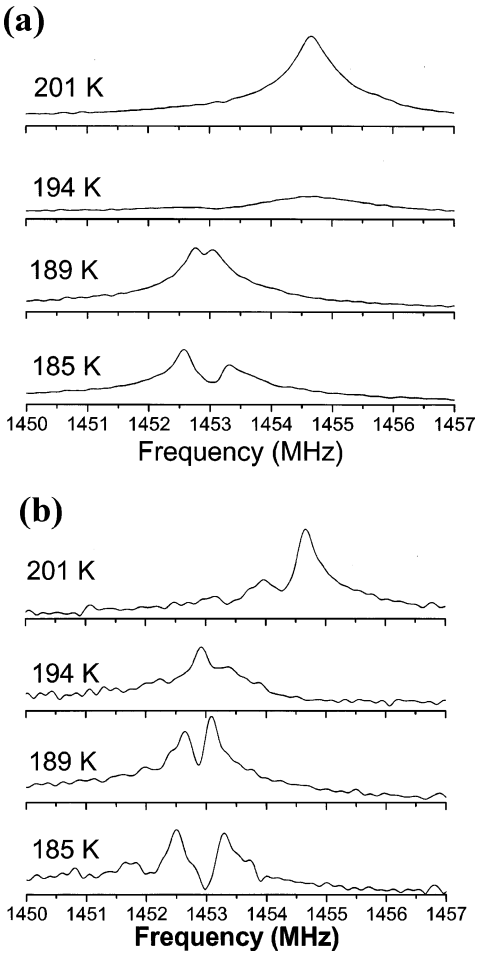

Figure 2. ZF EPR FID FT spectra of the T_x−T_z transition at temperatures above and below T_c (193 K) for (a) PHPT and (b) PDPT. These spectra are 2D plots of Figure 1 at selected temperatures.

To make a proper comparison, we display the T_x−T_z transition frequencies for PHPT as a function of temperature in Figure 4 which includes our data and Kohler's results at 1.2 K.[17] Before we proceed with our analyses, we note that the observed spectroscopic sites are named as O_1 through O_4 in optical studies and in ODMR experiments. The frequencies of the low-frequency peaks (1452−1454 MHz) in Figure 3 are close to those of O_3 and O_4 measured at 1.2 K (1456−1459 MHz). We therefore propose that the low-frequency peaks correspond to O_3 and O_4, whereas the high-frequency peaks correspond to O_1 and O_2. This assignment is corroborated by

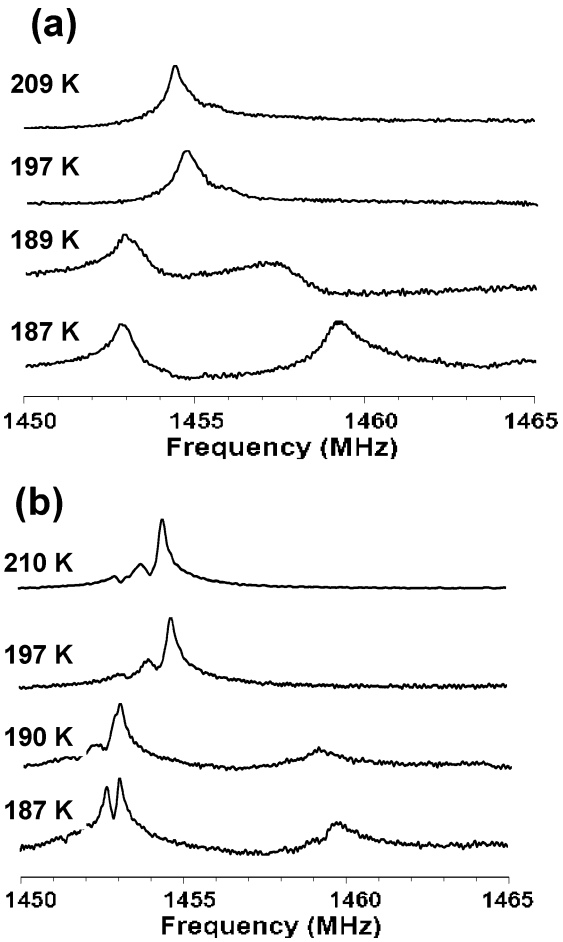

Figure 3. ZF spectra of the T_x-T_z transition at temperatures above and below T_c (193 K) for an extended spectral region of (a) PHPT and (b) PDPT. A different crystal sample was used in these measurements.

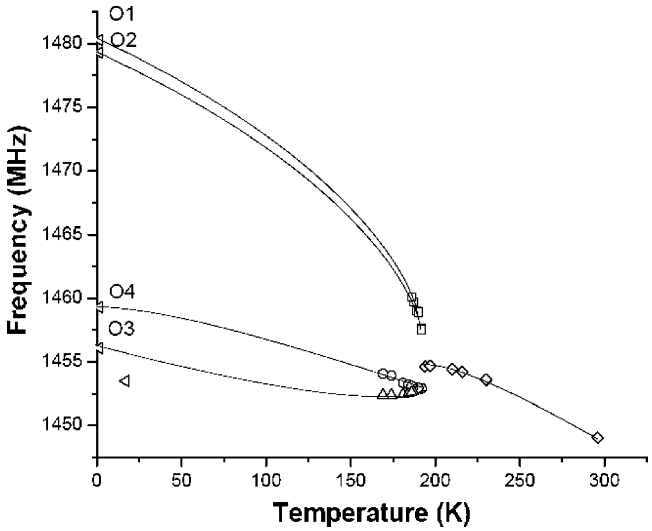

Figure 4. Observed T_x-T_z transition frequencies for PHPT as a function of temperature.

the observation that the weak high-frequency peak shifts to a higher frequency at a rate of 300 kHz per deg of temperature change when the temperature decreases within the range from (T_c − 10 K) to T_c. The change of transition frequency is expected to be continuous between T_c and 1.2 K, and the continuation of the fast shifting trend of the high-frequency peak allows alignment with (O_1/O_2), as indicated in Figure 4. Also note that the frequency difference between (O_3/O_4) and (O_1/O_2) is 3.2 and 1.0 MHz, respectively, at 1.2 K; we observed that the low-frequency group consists of two peaks because it has a large enough splitting, and the weak high-frequency group does not have two distinguishable peaks. This is especially clear as shown in Figure 3 for PDPT. Therefore, we assign the strong low-frequency peaks to spectroscopic sites (O_3/O_4) and the weak high-frequency peaks to (O_1/O_2).

TABLE 1: Distances between the Pentacene Molecular Center and the Nearest Host Protons

crystal site	distance, Å[a]
M_1	3.0
M_2	4.0
M_3	3.1
M_4	3.6
monoclinic M_0	3.5

[a] Precisions of the distance values are 0.1 Å, assuming that the 3D modeling software (Chem3D) has precision that is better than 0.1 Å.

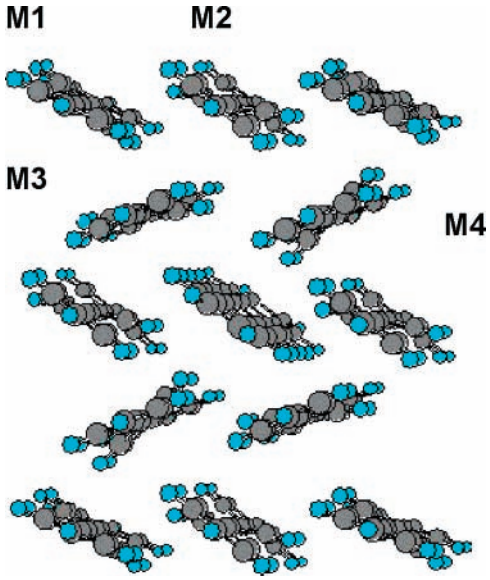

Figure 5. Pentacene that has been doped in *p*-terphenyl triclinic crystal at the center of the cell has projected onto the *ab* cleavage plane and occupies an M_1 crystal site. The unit cell was built based on the parameters given in ref 1. The blue dots are hydrogen atoms and the grey ones are carbon atoms. The pentacene molecule is depicted as planar. Crystal sites M_1 through M_4 are identified by the inter-ring torsional angle, which is documented in ref 12.

To gain some insight into the molecular packing of the crystal lattice, we built a 3D model of pentacene molecules that occupy four different crystal sites, M_1-M_4, and "measured" the distances between the nearest host protons and the pentacene molecular centers, as listed in Table 1 (see Figure 5 for $M_1\cdots M_4$ notation). Here we assumed that the pentacene molecule has the same orientation as the replaced *p*-terphenyl molecule (M_1 site), with the long-axis (*x*) of the pentacene parallel to the long-axis of the *p*-terphenyl and the short-axis (*y*) orthogonal to *x* and parallel to the outer phenyl ring plane of *p*-terphenyl. As one notes that the pentacene molecules in sites M_1 and M_3 are closer to their nearest host protons than pentacene molecules in other triclinic and monoclinic sites.[12] Because the distances between the pentacene molecular center and the immediately adjacent host atoms are related to the calculated pentacene conformation based on molecular packing, it is most likely that (M_1/M_3) correspond to the two nonplanar conformations, whereas (M_2/M_4) correspond to the planar conformations. In fact, Kryschi et al. showed that the equilibrium conformations

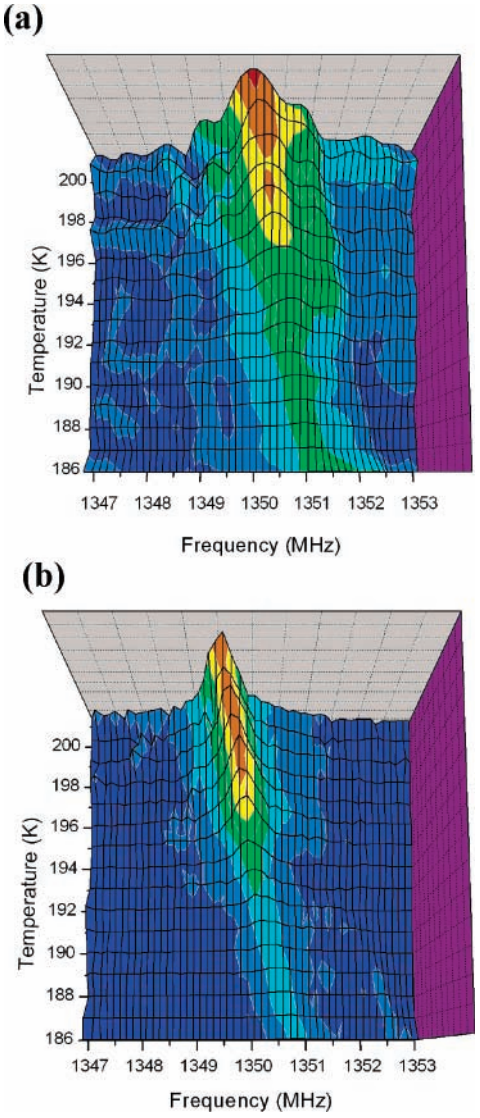

Figure 6. ZF spectral assemblies of the T_y-T_z transition at temperatures near T_c for (a) PHPT and (b) PDPT.

of pentacene molecules in two of the four triclinic sites are similar to that of pentacene molecules in monoclinic sites (i.e., nearly planar), whereas molecules in the other two triclinic sites are nonplanar.[11] Bordat et al. also reached a similar conclusion that pentacene in (M_1/M_3) are nonplanar and that those in (M_2/M_4) are nearly planar based on a different molecular dynamics model.[19]

Furthermore, the differences of zero-field splitting (ZFS; hence, different ZF transition frequencies) among pentacene molecules in different sites are likely due to molecular distortions caused by adjacent host molecules. From the molecular packing calculations, the nonplanar pentacene molecules have a lower symmetry and the triplet electrons are likely more localized than the planar molecules. Hence, the nonplanar molecules are likely (O_1/O_2), which have a larger ZFS, and the planar molecules are likely (O_3/O_4). Therefore, we made the following assignments between the crystal sites and the spectroscopic site: (M_1/M_3) ↔ (O_1/O_2) and (M_2/M_4) ↔ (O_3/O_4).

Moreover, the weak high-frequency peak of the T_x-T_z transition, which we assigned to (O_1/O_2), has a large blue shift as the temperature cools down further. This blue shift is the likely result of the gradual increase of the torsional angle between the *p*-terphenyl central and the outer phenyl rings for the following reason:[1,24] a larger torsional angle means more "intrusive" central phenyl rings near sites (M_1/M_3), which may distort pentacene molecules further from planarity and increase ZFS and T_x-T_z transition frequencies. Furthermore, the nonplanar pentacene molecules are likely to increase the T_z population and reduce the T_x population due to the loss of symmetry[25] that may also account for the disappearance of spectral intensity at T_c as previously described. Consequently, a smaller population difference between the T_x and the T_z states will reduce the signal intensity of the T_x-T_z transition. This is consistent with the observation that the high-frequency group, ascribed as (O_1/O_2), has weaker signal intensity.

TABLE 2: PHPT T_x-T_z and T_y-T_z Transition Frequencies ZFS (in MHz) of Inequivalent Triclinic Sites[a]

	T_x-T_z	T_y-T_z	D	E
Köhler's work (1.2 K, ref 17)				
O_1	1480.3	1363.2	1421.7	−58.5
O_2	1479.3	1360.0	1419.7	−59.7
O_3	1456.1	1359.3	1407.7	−48.4
O_4	1459.3	1358.3	1408.8	−50.5
This work (182 K)				
$O_1{}^b/O_2{}^b$	1459.8[c]	1352.6[c]	1406.2	−53.6
$O_3{}^b$	1452.5	1351.5	1402.0	−50.5
$O_4{}^b$	1453.4	1351.5	1402.5	−51.0

[a] In MHz. [b] Note: proposed name assignment. [c] 187 K.

3. The Spectral Behaviors of the T_y-T_z Transition. The ZF spectral assemblies for the T_y-T_z transition of both PHPT and PDPT samples at temperatures around T_c are shown in Figure 6. We note that the S/N ratio for the T_y-T_z transition is less than that for the T_x-T_z transition as described above due to a smaller population difference between the T_y and the T_z sublevels. However, we observed a spectral broadening in this transition but not a distinct splitting as the temperature was decreased below T_c. This is consistent with a previous ODMR study at 1.2 K, where it was reported that the frequency differences for the T_y-T_z transition among different sites are not large enough to be resolvable.[17]

Because the measured T_y-T_z transition frequency differences between PHPT and PDPT are less than 0.8 MHz and their spectral patterns are similar, we shall neglect the differences between PHPT and PDPT in our discussion. Table 2 summarizes the T_x-T_z and the T_y-T_z transition frequencies, ZFS of PHPT measured at 182 and 187 K, and the Köhler's values measured at 1.2 K. These assignments are also consistent with Ong's x-band EPR results measured at 26 K.[8] Because we observed that at low temperatures the transition frequency shifts lower but does not split, we therefore could not make an assignment of spectroscopic sites. We thus rely on the measurements of the T_x-T_z transition for assignments as described in the last section.

Conclusions

Applying modern ZF EPR FID FT techniques and simple 3D molecular modeling allowed us to examine the spectral behaviors of the guest pentacene molecule dispersed in the *p*-terphenyl host crystal over a wide range of temperatures, especially at the T_c of the host crystal. These studies enable us to examine the effects of the dynamics and the structural changes of the host crystal onto the guest pentacene molecules. We further propose a unique spectral assignment regarding the molecular planarity of the pentacene molecule at low temperatures, which are consistent with previous theoretical and optical studies.

Acknowledgment. We wish to thank Professors Sam I. Weissman and Ronald Lovett for helpful discussion. This work

is supported in part by the Petroleum Research Fund, administrated by the American Chemical Society (No. 36970-AC5).

References and Notes

(1) Baudour, J. L.; Cailleau, H.; Yelon, W. B. *Acta Crystallogr.* **1977**, *B33*, 1773.
(2) Rietveld, H. M.; Maslen, E. N.; Clews, C. J. B. *Acta. Crystallogr.* **1970**, *26*, 693.
(3) Baudour, J. L.; Delugeard, Y.; Cailleau, H. *Acta. Crystallogr.* **1976**, *B32*, 150.
(4) Moerner, W. E.; Carter, T. P. *Phys. Rev. Lett.* **1987**, *59*, 2705.
(5) Orrit, M.; Bernard, J. *Phys. Rev. Lett.* **1990**, *65*, 2716.
(6) Reilly, P. D.; Skinner, J. L. *J. Chem. Phys.* **1995**, *102*, 1540.
(7) Yang, T. C.; Sloop, D. J.; Weissman, S. I.; Lin, T.-S. *J. Chem. Phys.* **2000**, *113*, 11194.
(8) Ong, J.-L.; Sloop, D. J.; Lin, T.-S. *J. Phys. Chem.* **1993**, *97*, 7833.
(9) Yu, H.-L.; Lin, T.-S.; Weissman, S. I.; Sloop, D. J. *J. Chem. Phys.* **1984**, *80*, 102.
(10) Lin, T.-S. *Chem. Rev.* **1984**, *84*, 1.
(11) Kryschi, C.; Fleischhauer, H. C.; Wagner, B. *Chem. Phys.* **1992**, *161*, 485.
(12) Güttler, F.; Croci, M.; Renn, A.; Wild, U. P. *Chem. Phys.* **1996**, *211*, 421.
(13) Meyling, J. H.; Wiersma, D. A. *Chem. Phys. Lett.* **1973**, *20*, 383.
(14) Patterson, F. G.; Lee, H. W. H.; Wilson, W. L.; Fayer, M. D. *Chem. Phys.* **1984**, *84*, 51.
(15) Orlowski, T. E.; Zewail, A. H. *J. Chem. Phys.* **1979**, *70*, 1390.
(16) Williams, J. O.; Jones, A. C.; Davies, M. J. *J. Chem. Soc. Faraday Trans. II* **1983**, *79*, 263.
(17) Köhler, J.; Brouwer, A. C. J.; Groenen, E. J. J.; Schmidt, J. *Chem. Phys. Lett.* **1996**, *250*, 137.
(18) Fleischhauer, H. C.; Kryschi, C.; Wagner, B. *J. Chem. Phys.* **1992**, *97*, 1742.
(19) Bordat, P.; Brown, R. *Chem. Phys. Lett.* **1998**, *291*, 153.
(20) Lang, J.; Sloop, D. J.; Lin, T.-S. *J. Magn. Reson.* **2005**, *176*, 249.
(21) Lang, J. Pulsed EPR Studies of Pentacene Triplet State in Zero and Near Zero Magnetic Field from 300 to below Phase Transition Temperature of *p*-Terphenyl. Ph.D. thesis, Washington University in St. Louis, 2005.
(22) Gullion, T.; Conradi, M. S. *Phys. Rev. B* **1984**, *30*, 1133.
(23) Gullion, T.; Conradi, M. S.; Rigamonti, A. *Phys. Rev. B* **1984**, *31*, 4388.
(24) Cailleau, H.; Baudour, J.-L.; Meinnel, J.; Dworkin, A.; Moussa, F.; Zeyen, C. M. E. *Faraday Discuss. Chem. Soc.* **1980**, *69*, 7.
(25) Clarke, R. H.; Frank, H. A. *J. Chem. Phys.* **1976**, *65*, 39.